

## **MODELS OF SPHERULITE GROWTH AND STRUCTURE BASED UPON TESSELLATIONS**

**Roman Čermák and Petr Ponižil**  
**Tomas Bata University in Zlin, Faculty of Technology**  
**TGM 275, 762 72 Zlín**  
**Czech Republic**

### **ABSTRACT**

*In this work, the modelling of growth and final structure of spherulites in thin polymer layer using planar tessellations is introduced. For these purposes, polypropylene film was fixed between two slides and isothermal-crystallized in a hot-stage microscope. The whole crystallization was scanned using camera. Images of both growing and final spherulitic structures were compared with the growing models of planar tessellations. It was found that the non-homogeneous Johnson-Mehl tessellation represents the most reliable model of the spherulitic structure in thin polymer layer. However, the final structure of spherulites can be sufficiently modelled by simpler tessellations, i.e. Poisson-Voronoi tessellation and homogeneous Johnson-Mehl tessellation.*

### **1. INTRODUCTION**

Spherulites are an ubiquitous form of crystal aggregate, found in a diverse range of fundamentally different materials, e.g. in viscous magmas [1] and laminar crusts [2], in vitamins and red blood cells [3], and in a wide range of industrially important thermoplastic polymers [4]. They are also found in thin films of water, in salts that have been crystallized from thickened solutions [5], and in many other systems. The essential features of spherulitic crystallisation are the same across this wide diversity of substances. Spherulites are spherical aggregates of anisotropic crystals that grow from a common, central, nonspherical, sheaf like aggregate.

Recently, studies of spherulites have concentrated mainly on polymer systems where they are frequently found forms of crystal growth from the melt or from dilute solution. In the latter case, polymer chains fold back upon themselves to form s.c. “lamellar” crystals of the thickness approx. 10–20 nm [6] and the degree of ordering within lamellae is dependent on the crystallisation conditions. In the former case, a less ordered system with more or less separated chains is created.

### **2. THEORY**

The starting point of the theory is the *Johnson-Mehl* model of radial growth from germs (nuclei). The germs are a realisation of a stationary point process in the  $(d + 1)$ -dimensional half-space  $\mathbf{R}^d \times \mathbf{R}_+$  ( $d = 2$  in the planar case of thin spherulite layers). The isotropic growth rate  $v$  is constant (a more general model with a variable rate  $v(t)$  is mathematically intractable) and the growth continues until growing nucleus meets an adjacent grain. The intensity measure  $\Lambda(dt)$  (number of nuclei born at time  $t$  per the time interval  $dt$ ) is  $I(t)dt$  and there is an additional condition, namely that a nucleus born within an already growing grain is rejected. Hence the nucleation proceeds on the uncovered area and the total number  $dN$  of nuclei born in an area  $W$  and retained within the time interval  $dt$  is  $W p(t) I(t) dt$ , where  $p(t)$  is the probability that a nucleus is accepted and  $1 - p(t)$  is the area fraction of already grown spherulites. The intensity of spherulites at the time  $t$  is then [7]

$$\lambda(t) = \int_0^t p(t)I(t)dt \quad (1)$$

and the observable rate of the process intensity is

$$\frac{d\lambda}{dt} = I(t)p(t) \quad (2);$$

the common and tractable assumption is

$$I(t) = \alpha t^{\beta-1}, \alpha > 0, \beta > 0 \quad (3).$$

The dispersion of grain sizes increases with the growing  $\beta$ . Consequently, the variances of grain characteristics (area  $a$ , perimeter  $p$  and edge number  $n$ ) increase, their mean values decrease. The grain boundaries are curved in the both Johnson-Mehl models, as the radii of impinging grains are different.

If  $\beta \rightarrow 0$ , then the Johnson-Mehl tessellation approaches the well-known stationary (convex polygonal) *Poisson-Voronoi tessellation* (PVT). The standard Voronoi tessellation [8] represents isotropic simultaneous radial growth with constant rate  $v$  from germs arranged arbitrarily whereas germs are a realisation of the Poisson point process in PVT. If  $\alpha = \text{const.}$ , the birth rate is time independent, the tessellation is called the *homogenous JM* model and the probability

$$p(t) = e^{-\frac{\pi\alpha v^2 t^3}{3}} \quad (4).$$

### 3. EXPERIMENTAL

Five equivalent foils were prepared by the crystallisation from xylene solution of the Mosten 58.412 isotactic polypropylene supplied by Chemopetrol Litvínov, Czech Republic. The material can be characterized by following properties: grade 58.412, melt flow index 2.5–4.0 g/10 min, density 900–910 kg/m<sup>3</sup>. The polypropylene was diluted in xylene at the 130 °C and the temperature was held within the interval 100–130 °C until the complete evaporation of the xylene which resulted in the formation of a foil of thickness (50 ± 5) µm on the flat bottom of the vessel. A sample of 5mm in diameter was then cut from the foil and thermally treated in the hot-stage microscope. The temperature cycle was as follows: 20 °C → 40 °C/min → 200 °C, 5 min (the complete melting attained) → -10°C/min → 124 °C. The crystallisation proceeding at the temperature 124 °C was observed and scanned. The scanning started after the first nuclei of spherulite were observed ( $t = 0$ ).

The pictures were taken after either 60 s ( $t \leq 240$  s) or 120 s ( $t > 240$  s). The microphotographs of the sampled area ( $W = 3 \text{ mm}^2$ ) were scanned with the resolution 500 DPI (total magnification 325 pixels/mm of the sample) and further processed digitally. The sequence of observations made the estimation of the number of nuclei  $N(t)$  as well as of the area fraction  $A_A(t) = 1 - p(t)$  possible (the point method was used). The total number of spherulite grains in each sample is shown in Table 1.

## 4. RESULTS AND DISCUSSION

### 4.1. Nucleation

By Eq. (1), the birth intensity  $I(t)$  can be estimated as

$$[I(t')]_{p(t')} = \frac{\Delta N(t)}{W\Delta t} \frac{1}{[p(t')]_{A_A}}, t' \in \Delta t = t_2 - t_1 \quad (5),$$

$$\Delta N(t) = N(t_2) - N(t_1) \quad (6),$$

where

$$t' = \frac{(t_2 - t_1)}{2} \quad (7),$$

$$[p(t')]_{A_A} = \frac{(2 - A_A(t_2) - A_A(t_1))}{2} \quad (8)$$

and  $A_A(t)$  is the area fraction of spherulites. The assumption of Eq. (3) gives

$$\ln[I(t)]_{p(t)} = \ln \alpha + (\beta - 1) \ln t \quad (9).$$

Hence the parameters  $\alpha$  and  $\beta$  can be estimated by linear regression; the value of  $\tau = t' - t_0$  should be inserted for  $t$ , where  $t_0 < 0$  is the estimate of the time elapsed from the true start of the crystallisation (for its estimation see below). The sample C was the most suitable for a detailed examination and the estimates

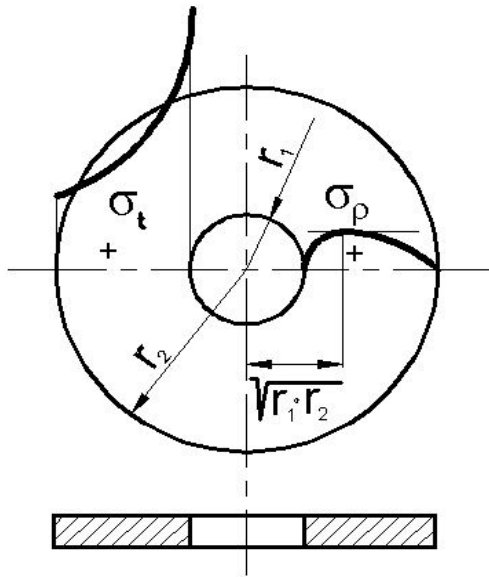


Figure 2 Stress progression in rotating wheel

$[I(t')]_{p(t)} \approx [\alpha]_{p(t),v} \approx 0.25-0.10 \text{ mm}^{-2}\text{s}^{-1}$  decreasing with the growing time were obtained from Eq. (5) and the hypothesis that the observed tessellation is homogenous JM model can be rejected. Limiting the regression to the first four values of  $\Delta N$ , reasonable values of  $[\alpha] = 2.0$ ,  $[\beta] = 0.39$  were obtained from Eq. (9).

#### 4.2. Spherulite growth

One sufficiently sizeable spherulite has been selected in each sample and its growth (radius  $r(t)$ ) was followed. Linear isotropic radial growth was observed in the all five cases with the approximately constant growth rates 0.25–0.26 and 0.21 mm/s (sample C). By extrapolating to  $r = 0$  the observed linear relation  $r = v(t - t_0)$ , an upper bound of the beginning of the recrystallisation  $t_0$  was found for each sample.

#### 4.3. Final structure

Number of examined grains, comparison of the sample mean values of spherulite grain characteristics and their sample variances with the values appropriate for Poisson-Voronoi tessellation and homogeneous Johnson-Mehl model are listed in Table 1. The mean values and variances of spherulite structure predominantly lie in between the values appropriate for PVT and JM model thus confirming the above hypothesis concerning the value of  $0 < \beta < 1$ .

Table 1. Characteristics of real spherulite structure, Poisson-Voronoi tessellation and homogeneous Johnson-Mehl model.

• sample	number of grains	number of edges		perimeter		area	
		$E n$	$\text{var } n$	$E p$	$\text{var } p$	$E a$	$\text{var } a$
PVT	-	6.000	1.78	4.000	0.95	1.00	0.280
A	127	6.008	1.71	3.961	0.86	1.00	0.227
B	85	5.905	2.39	3.785	1.95	1.00	0.571
C	73	5.822	1.93	3.852	1.59	1.00	0.448
D	66	6.091	1.87	3.861	1.36	1.00	0.384
E	66	5.894	2.18	3.879	1.37	1.00	0.486
JM model	-	6.000	5.92	3.734	3.52	1.00	0.703

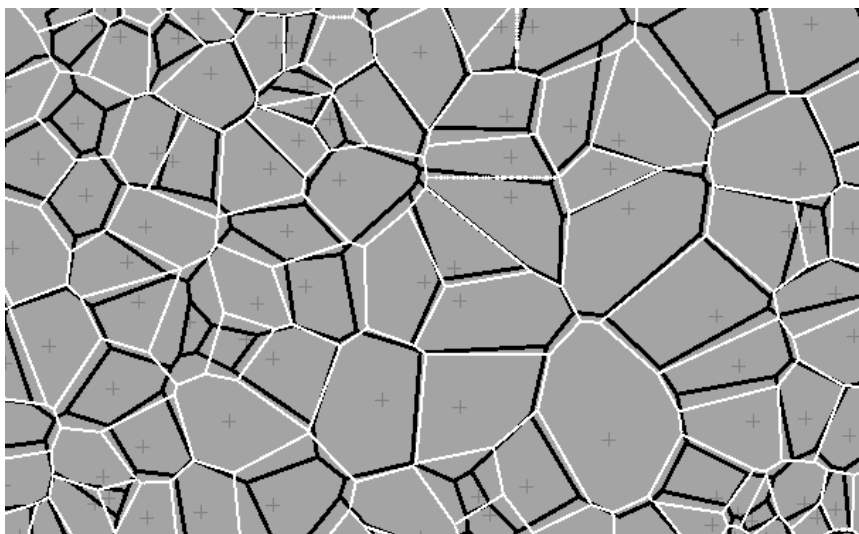


Figure 1. Comparison of final spherulite structure (black lines) of sample B and Voronoi tessellation (white lines) based on the same generators, i.e. real spherulitic nuclei (grey cross symbols).

The final spherulite structure was compared with the Voronoi and Johnson-Mehl tessellations based on the same systems of generators, i.e. real spherulitic nuclei. Examples of these comparisons are shown in Figures 1 and 2. As can be seen, in both cases the real and modelled structures displays satisfactory coincidences. In particular, the Johnson-Mehl tessellation represents an outstanding model of real 2D spherulite structure.

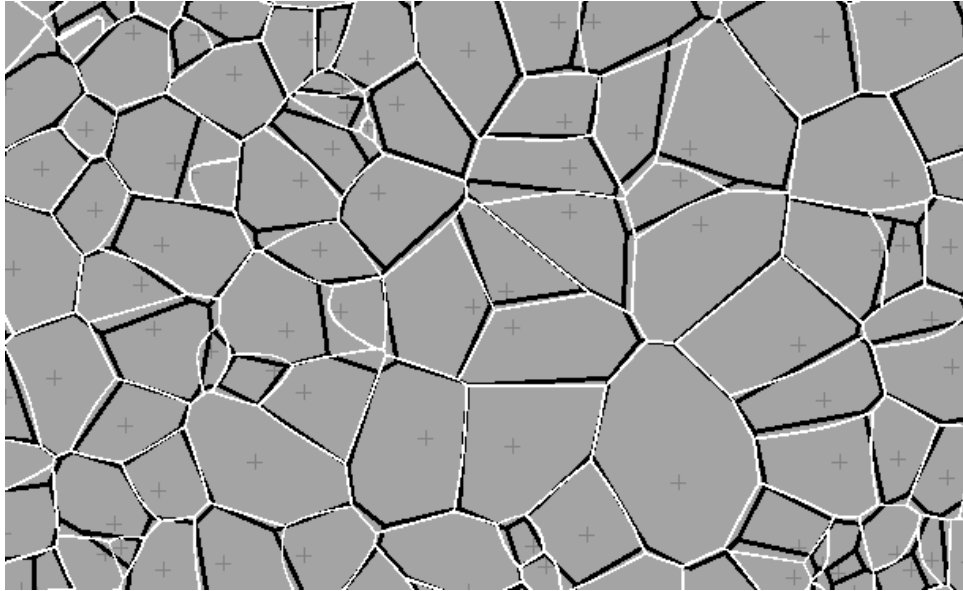


Figure 2. Comparison of final spherulite structure (black lines) of sample B and Johnson-Mehl tessellation (white lines) based on the same generators, i.e. real spherulitic nuclei (grey cross symbols).

## 5. CONCLUSIONS

In the observed tessellation produced by spherulites, the spherulite area distribution in the sample A differed from those ones in the remaining samples but all samples approximately coincided after the renormalisation to the unit mean area. The obtained values of area  $a$ , perimeter  $p$  and edge number  $n$  together with the corresponding variances are compared with the theoretical and simulation based values of the unit PVT and homogeneous JM model. The mean values and variances predominantly lie just between the values appropriate for PVT and JM model thus confirming the above hypothesis concerning the value of  $0 < \beta < 1$ . In addition, the Johnson-Mehl tessellation based on the real system of generators represents an outstanding model of 2D spherulite structure.

## 6. ACKNOWLEDGEMENTS

The authors kindly acknowledge the support provided from the Ministry of Education, Youth and Sport of the CR (project MSM7088352101) and the Czech Science Foundation (project 106/05/0550).

## 7. REFERENCES

- [1] Colburn R., The Formation of Thundereggs. <http://www.zianet.com/geodekid/thndregg.htm> (1998)
- [2] Larkin SP, Levander A, Henstock TJ, Pullammanappallil S. Is the Moho flat? Seismic Evidence for a Rough Crust-mantle Interface Beneath the Northern Basin and Range to Geology, Geol Soc Amer, 25, 385 (1997)
- [3] Streekstra GJ, Hoekstra AG, Nijhof EJ, Heethaar RM. Light Scattering by Red Blood Cells in Ektacytometry: Fraunhofer Versus Anomalous Diffraction. Appl Opt, 32, 2266 (1993)
- [4] Remaly LS, Schultz JM. Time-Dependent Effect of Spherulite Size on the Tensile Behavior of Polypropylene. J Appl Polymer Sci, 14, 1871 (1970)
- [5] McHugh AJ, Schultz JM. Extensional Flow Induced Crystallization from Solution, Kolloid-Zeitschrift, 251, 193 (1973)
- [6] Meissner B, Zilvar V. Fyzika polymerů. Praha: SNTL/ALFA (1987)
- [7] Møller J. Random Johnson - Mehl Tessellations. Adv Appl Prob, 24, 814 (1992)
- [8] Okabe A, Boots B, Sugihara K. Spatial Tessellations. Chichester: J. Wiley & Sons (1992)